

# Instability versus nonlinearity in certain nonautonomous oscillators: A critical dynamical transition driven by the initial energy

C. Degli Esposti Boschi<sup>1,3,\*</sup> and L. Ferrari<sup>1,2,†</sup><sup>1</sup>*Istituto Nazionale per la Fisica della Materia—Unità di Bologna, viale Berti-Pichat, 6/2, 40127, Bologna, Italy*<sup>2</sup>*Dipartimento di Fisica dell'Università di Bologna, viale Berti-Pichat, 6/2, 40127, Bologna, Italy*<sup>3</sup>*Departamento de Física Aplicada, Universidad de Alicante, Apartado 99, 03080, Alicante, Spain*

(Received 2 August 2000; published 26 January 2001)

The equation of motion  $\ddot{q} + \Omega^2(t)q + \alpha|q|^{\gamma-2}q = 0$  ( $\gamma > 2$ ) for the real coordinate  $q(t)$  is studied, as an example of the interplay between nonlinearity and instability. Two contrasting mechanisms determine the behavior of  $q(t)$ , when the time-varying frequency  $\Omega(t)$  does produce exponential instability in the linear equation  $\ddot{q}_{\text{lin}} + \Omega^2(t)q_{\text{lin}} = 0$ . At low energy, the exponential instability is the dominant effect, while at high energy the bounding effect of the autonomous nonlinear term prevails. Starting from low initial energies, the result of this competition is a time-varying energy characterized by quasiperiodic peaks, with an average recurrence time  $T_{\text{peak}}$ . A closed critical curve  $S_\omega$  exists in the initial phase space, whose crossing corresponds to a divergence of the recurrence time  $T_{\text{peak}}$ . The divergence of  $T_{\text{peak}}$  has a universal character, expressed by a critical exponent  $a=1$ . The critical curve  $S_\omega$  is the initial locus of the solutions that vanish asymptotically. A close relationship exists between this dynamical transition and the transition from mobile to self-trapped polarons in one spatial dimension. The application to a number of physical problems is addressed, with special attention to the Fermi-Pasta-Ulam problem and to transitions to chaos.

DOI: 10.1103/PhysRevE.63.026218

PACS number(s): 05.45.-a, 64.60.Ht, 02.30.Hq

## I. INTRODUCTION

In a recent paper [1] the authors addressed the interplay between nonautonomous and nonlinear effects for *generalized* classical oscillators, i.e., systems described by one real degree of freedom  $q(t)$ , that move back and forth about a stable (and unique) equilibrium position. The main result was as follows: for a wide class of generalized oscillators, with a time-dependent Hamiltonian, the presence of an *autonomous* term, diverging more than quadratically with the coordinate, is a sufficient condition for the boundedness of all solutions. This result is especially relevant if one considers the Hamiltonian

$$H_{\text{lin}} = \frac{p^2 + \Omega^2(t)q^2}{2} \quad (1)$$

of a linear oscillator with a time-fluctuating square frequency  $\Omega^2(t)$  [2]. In case (1), there exist conditions of *exponential instability* (EI), such that  $q(t)$  has an *exponentially diverging* envelope  $\exp(\omega t)$ , with rate  $\omega > 0$  [1,3–5]. However, under the same conditions, the Hamiltonian

$$H = H_{\text{lin}} + \frac{\alpha}{\gamma}|q|^\gamma = \frac{p^2 + \Omega^2(t)q^2}{2} + \frac{\alpha}{\gamma}|q|^\gamma \quad (\gamma > 2, \alpha > 0, \dot{\alpha} = 0), \quad (2)$$

yields a bounded solution, even for *arbitrarily small* values of the positive parameter  $\alpha$ . Therefore, the nonlinear term in the equation of motion

$$\ddot{q} + \Omega^2(t)q + \alpha|q|^{\gamma-2}q = 0 \quad (3)$$

cannot be treated as a perturbation, whenever EI conditions are satisfied by the linear part. In particular, the bounded function  $q(t; \alpha)$  will approach an exponentially unstable solution *nonuniformly* in time, when  $\alpha$  tends to zero. Equation (3) is actually the simplest possible case for studying the interplay between EI and nonlinearity in a nonperturbative way.

In many physical cases, Eq. (1) can be regarded as a zero-order approximation, while Eq. (2) represents a natural generalization, including higher-order terms. The example of an elastic horizontal bar, stressed by longitudinal time-varying forces [4], was used in Ref. [1] as a physical application concerned with safety-control systems. Here we recall that the interplay between EI and nonlinearity can address a number of further applications, like the *squeezing* of photons [6–9] or phonons [10] and the *confinement* of charged particles (beams in accelerators [11–15] and Paul traps [16]). Hence the results of the present paper are relevant to many physical problems, ranging from atomic-molecular to macroscopic length scales. A possible application to the Fermi-Pasta-Ulam problem [17,18] will be considered in Sec. IX.

From now on, it is explicitly assumed that the EI conditions are satisfied for  $H_{\text{lin}}$ . In the next sections we study Eq. (3), both analytically and numerically. The main results are as follows:

(i) *Vanishing and BOWL solutions*: There are solutions [denoted as  $q_\omega(t)$ ] that *vanish* asymptotically, with envelope

\*Electronic address: esposti@ua.es

†Electronic address: ferrari@df.unibo.it

$\exp(-\omega t)$ .  $q_\omega(t)$ 's are the *only* possible vanishing solutions. The corresponding set of initial values  $(\dot{q}_i, q_i)$  is a *closed* curve  $S_\omega$  in the phase-space plane. Apart from  $S_\omega$ , all the solutions are *bounded and oscillating without limit* (BOWL solutions). The maximum energy achievable by the vanishing solutions is *bounded from above* by a value  $E_0$ . The maximum energy achievable by the BOWL solutions is *bounded from below* by a value  $E_{\text{inf}} > 0$ . Both  $E_0$  and  $E_{\text{inf}}$  are independent from the initial conditions.

(ii) *BOWL solutions at low energy*: If the initial energy  $E_i$  is small compared to a certain characteristic scale  $E_l$ , the energy of the BOWL-solutions exhibits an almost periodic sequence of peaks, centered around instants  $\{T_n, n = 1, 2, \dots\}$ . The peaks' shape is well described by the expression  $E_{\text{Max}} \exp[2\omega(t - T_n)]$ ,  $E_{\text{Max}}$  being the maximum energy attained. The mean value of the peak-to-peak recurrence time turns out to be  $T_{\text{peak}} \cong \omega^{-1} \ln(E_{\text{Max}}/E_i)$ , at low initial energy.

(iii) *Critical dynamics*: The behavior of the BOWL solutions is singular, when the initial conditions tend to any point of the curve  $S_\omega$  (the initial locus of the vanishing solutions). The singularity is *universal*, and results in a divergence of the peak-to-peak correlation time  $T_{\text{peak}}$ . Therefore, the BOWL-to-vanishing transition is a critical process, driven by the initial conditions  $\vec{z}_i \equiv (\dot{q}_i, q_i)$ . The curve  $S_\omega$  is the locus of the "critical points"  $\vec{z}_c$  of the transition. The quantity  $R \equiv |E_i - E_c|/E_c$  can be taken as the "relevant field,"  $E_c(\vec{z}_c)$  being any initial energy attained by a vanishing solution. On defining  $\exp(\omega T_{\text{peak}})$  as the "correlation length," the "principal critical exponent" of the transition turns to be  $a = 1$ , i.e.,  $\exp(\omega T_{\text{peak}}) \propto R^{-1}$ .

(iv) *BOWL solutions at high energy*: If the initial energy  $E_i$  is large compared to a certain characteristic scale  $E_h$ , the fluctuating part  $\Omega_0^2 \xi(t)$  of the square frequency

$$\Omega^2(t) = \Omega_0^2 [1 + \xi(t)], \quad \Omega_0^2 = \lim_{t \rightarrow \infty} \frac{1}{t - t_i} \int_{t_i}^t dt' \Omega^2(t') \quad (4)$$

can be treated as a *perturbation*, and the solution  $q(t)$  can be expressed as  $q_0(t) + O(\xi; t)$ . The unperturbed part  $q_0(t)$  satisfies the *autonomous*, nonlinear equation

$$\ddot{q}_0 + \Omega_{\text{eff}}^2 q_0 + \alpha |q_0|^{\gamma-2} q_0 = 0, \quad (5)$$

where  $\Omega_{\text{eff}}^2$  is an effective square frequency, to be determined self-consistently. The symbol  $O(x; y)$  is used, here and in what follows, to indicate a function vanishing *at least* linearly in  $x \rightarrow 0$  and uniformly in  $y$ . Hence, in the high-energy regime, the energy is conserved, apart from relatively small fluctuations just above the initial value  $E_i$ .

(v) *Chronological humps and self-trapped polarons*: The equation of motion (3) can be mapped into the eigenvalue equation for a *quantum polaron* in one spatial dimension. A *self-trapped* polaron is a quantum solution localized in space, and vanishing exponentially at  $\pm\infty$ . The classical analog is a solution of Eq. (3) that starts with zero amplitude at  $t = -\infty$ , attains a maximum amplitude at a finite time, then vanishes again at  $t = +\infty$ . We call this solution of the nonlinear

oscillator [Eq. (3)] a *chronological hump*. It is shown that the BOWL solutions at low energy can be regarded as a sequence of "correlated" chronological humps. Accordingly, the BOWL-to-vanishing transition can be described as an infinite-scale correlation of the chronological humps. Due to the analogy between Eq. (3) and the quantum polaron problem, the universal properties addressed in point (iii) apply to the *mobile-to-self-trapped polarons* transition as well.

## II. AN INTEGRAL REPRESENTATION OF EQ. (3)

If  $\Omega^2(t)$  satisfies EI conditions, the general solution for Hamiltonian (1) can be written as

$$q_{\text{lin}}(t) = q_+ f_+(t) + q_- f_-(t), \quad f_\pm(t) = u_\pm(t) \exp(\pm \omega t),$$

$$\dot{f}_+(t) f_-(t) - \dot{f}_-(t) f_+(t) = 1, \quad (6)$$

where the functions  $u_\pm(t)$  are *bounded and oscillating without limit* (BOWL functions). The condition in the second line ( $\text{Wr}=1$ ) is not necessary, but leads to some simplifications. The two constants  $q_\pm$  determine the arbitrary initial conditions for  $q_{\text{lin}}(t)$ . The Green-function method can be applied to the linear part of Eq. (3), by treating the nonlinear term as a given function of time. This makes it possible to write the equation of motion (3) in an integral form, whose solution has the same initial conditions as  $q_{\text{lin}}(t)$  at  $t = t_i$ :

$$q(t) = \left[ q_+ - \alpha \int_{t_i}^t dt' f_-(t') |q(t')|^{\gamma-2} q(t') \right] f_+(t)$$

$$+ \left[ q_- - \alpha \int_{t_i}^t dt' f_+(t') |q(t')|^{\gamma-2} q(t') \right] f_-(t). \quad (7)$$

From now on, we assume  $t \geq t_i$ , unless otherwise stated. On multiplying both sides of Eq. (7) by  $\exp(-\omega t)$ , then taking the limit  $t \rightarrow \infty$ , the boundedness of  $q(t)$  yields

$$q_+ \equiv \alpha \int_{t_i}^{\infty} dt f_-(t) |q(t)|^{\gamma-2} q(t) \quad (\text{identity}). \quad (8)$$

Note that expression (8) is just an *identity*, not an equation. In general, it does *not* determine a relation between the two constants  $q_\pm$ , unless such a relation does exist independently. On re-expressing Eq. (7) in terms of Eq. (8), one obtains another equivalent form of the equation of motion, in which the constant  $q_+$  is (seemingly) eliminated:

$$q(t) = q_- f_-(t) + \alpha \int_{t_i}^{\infty} dt' \phi(t, t') e^{-\omega|t-t'|} |q(t')|^{\gamma-2} q(t'), \quad (9a)$$

where

$$\phi(t, t') = \phi(t', t) = \begin{cases} u_+(t) u_-(t') & \text{for } t \leq t' \\ u_-(t) u_+(t') & \text{for } t \geq t'. \end{cases} \quad (9b)$$

The advantage of using Eqs. (9) instead of Eq. (3) is that the former contain explicitly the new time scale  $\omega^{-1}$ , i.e., the ‘‘signature’’ of the EI in the linear oscillator [Eq. (1)]. However, the integral equation (9a) does *not* determine, in general, a unique solution, since the value of the integral on the right-hand side of identity (8) can be fixed by the arbitrary constant  $q_+$ , independent of  $q_-$ .

### III. VANISHING SOLUTIONS

When looking for vanishing solutions of Eq. (3), one should first note that they are less and less sensitive to the nonlinear term, as time goes by. Asymptotically, one expects to approach a solution proportional to  $f_-(t)$  [Eq. (6)]. It is not difficult to prove that the envelope of *any* vanishing solution is, necessarily,  $\exp(-\omega t)$ . Furthermore, the expression  $q_- f_-(t)$  must be approached in the limit  $\alpha \rightarrow 0$  at *any* time. Equation (9a) itself suggests the general structure of the vanishing solutions. The integral term can indeed be treated as a *perturbation* of the first term on the right-hand side. It is obvious that the resulting solution [that we denote as  $q_\omega(t)$ ] will be asymptotically *vanishing*, with the same envelope  $\exp(-\omega t)$  as  $f_-(t)$  [Eq. (6)]. We thus introduce an expansion in powers of  $\alpha$ ,

$$q_\omega(t) = q_- f_-(t) + \sum_{n=1}^{\infty} \alpha^n q_n(t), \quad (10a)$$

where, for example,

$$q_1(t) = |q_-|^{\gamma-2} q_- \int_{t_i}^{\infty} dt' \phi(t, t') e^{-\omega|t-t'|} \times |f_-(t')|^{\gamma-2} f_-(t'). \quad (10b)$$

The constant

$$q_+ = \alpha |q_-|^{\gamma-2} q_- C_- [1 + O(\alpha; q_-)], \quad (11)$$

$$C_- \equiv \int_{t_i}^{\infty} dt |f_-(t)|^\gamma$$

[see Eqs. (10a) and (8)] is now determined *uniquely* by  $q_-$ . Accordingly, the set of initial conditions  $S_\omega$  corresponding to the  $q_\omega(t)$ 's is a *curve*, in the two-dimensional phase space of the oscillator. With the aid of Eqs. (6) and (7), one has

$$\dot{q}_\omega(t_i) = q_\omega(t_i) (\dot{f}_- / f_-)_{t_i} + q_+ / f_-(t_i) \quad [f_-(t_i) \neq 0], \quad (12)$$

and the curve  $S_\omega$  reads, from Eq. (11),

$$S_\omega \equiv \left\{ \vec{z}_i = (\dot{q}_i, q_i); \quad \dot{q}_i = q_i \left[ \frac{\dot{f}_-(t_i)}{f_-(t_i)} + \alpha \frac{|q_i|^{\gamma-2}}{|f_-(t_i)|^\gamma} \right] \right. \\ \left. \times C_- [1 + O(\alpha; q_i)] \right\} \quad [f_-(t_i) \neq 0]. \quad (13)$$

The quantity  $O(\alpha; q_i)$  originates from the power expansion (10a), and is defined only within a certain convergence ra-

dius. We are not able to calculate this convergence radius in general. However, in Sec. V we will show that the curve [Eq. (13)] is a *bounded* set, under suitable conditions on  $\Omega^2(t)$ . This implies that the convergence radius of Eq. (10a) is *finite*.

### IV. BOWL SOLUTIONS IN THE LOW-ENERGY REGIME

From the boundedness theorem proven in Ref. [1], it follows that any solution of Eq. (3) is either a vanishing or BOWL solution. Hence

$$S_{\text{Bowl}} = \mathbb{R}^2 - S_\omega \quad (14)$$

is the initial locus of the BOWL solutions. These are characterized by the property

$$q_\infty \equiv \lim_{t \rightarrow \infty} \sup_{(t, \infty]} \{|q(t)|\} > 0. \quad (15a)$$

Furthermore, one can always find a *monotonically decreasing* function  $M$  such that

$$|q(t)| < q_\infty [1 + M(t - t_i)], \quad \lim_{T \rightarrow \infty} M(T) = 0, \quad M(0) < \infty. \quad (15b)$$

In view of the discussion in what follows, let  $q = q(t; \vec{z}_i)$  express the dependence on the initial conditions  $\vec{z}_i = (\dot{q}_i, q_i)$ . From Eq. (15a), there exists an unbounded sequence  $\{t_m\}$  such that  $\lim_{m \rightarrow \infty} |q(t_m; \vec{z}_i)| = q_\infty(\vec{z}_i)$ . For each  $t_m$ , Eqs. (9a) and (15b) yield

$$|q(t_m; \vec{z}_i)| \leq |q_- f_-(t_m)| + \alpha \phi_M \int_{t_i}^{\infty} dt |q(t; \vec{z}_i)|^{\gamma-1} e^{-\omega|t_m-t|} \\ < |q_- f_-(t_m)| + \alpha \phi_M |q_\infty(\vec{z}_i)|^{\gamma-1} \\ \times \int_{t_i}^{\infty} dt [1 + M(t - t_i)]^{\gamma-1} e^{-\omega|t_m-t|}, \quad (16a)$$

where

$$\phi_M \equiv |\phi(t, t')|_{\text{Max}}. \quad (16b)$$

On taking the limit  $t_m \rightarrow \infty$  in Eq. (16a), it is seen that  $f_-(t_m)$  vanishes, and the integral in the last term tends to  $2\omega^{-1}$ , due to properties (15b) of the function  $M$ . Hence, recalling that  $\lim_{m \rightarrow \infty} |q(t_m; \vec{z}_i)| = q_\infty(\vec{z}_i)$ , one is left with the following lemma:

$$q(t) = \text{BOWL} \Rightarrow q_\infty(\vec{z}_i) > \left( \frac{\omega}{2\alpha\phi_M} \right)^{1/(\gamma-2)} \equiv Q^*. \quad (17)$$

Since  $Q^*$  is *independent of the initial conditions*, lemma (17) has an important consequence. Let  $q_{\text{Max}}(\vec{z}_i) \geq q_\infty(\vec{z}_i)$  be the maximum oscillator amplitude. Then

$$q_{\text{Max}}(\vec{z}_i) \geq \inf_{\{\vec{z}_i\}} q_\infty(\vec{z}_i) \geq Q^* > 0. \quad (18)$$

Or, equivalently, we have the following statement:

*Statement 1:* Under the EI conditions, the maximum amplitude  $q_{\text{Max}}(\vec{z}_i)$  and energy  $E_{\text{Max}}(\vec{z}_i)$  attainable by the BOWL solutions of Eq. (3) are both limited from below by strictly positive values  $q_{\text{inf}}$  and  $E_{\text{inf}}$ , independent of the initial conditions. It should be noticed that Statement 1 simply expresses the existence of  $q_{\text{inf}}$  and  $E_{\text{inf}}$ , whose explicit calculation, however, is not trivial.

The existence of BOWL solutions with *arbitrarily low* initial energy follows from Eq. (13), ensuring that it is always possible to take  $\vec{z}_i$  outside the curve  $S_\omega$ , with  $|\vec{z}_i|$  arbitrarily small. We address such BOWL solutions with special interest, because the point  $\vec{0}=(0,0)$  in the initial phase space is a special critical point for the BOWL-to-vanishing transition. The critical nature of the limit  $E_i \rightarrow 0$  follows from Eq. (17) and Statement 1, claiming that the BOWL function  $|q(t; \vec{z}_i)|$  must fit a value  $Q^* > 0$  independent of  $|\vec{z}_i|$ , even in the limit of vanishing  $|\vec{z}_i|$ . This might look inconsistent with the obvious requirement  $\lim_{|\vec{z}_i| \rightarrow 0} q(t; \vec{z}_i) = 0$  for each  $t$ . The solution of this apparent paradox is that in the limit  $E_i \rightarrow 0$  ( $|\vec{z}_i| \rightarrow 0$ ), the zero function  $q(t; \vec{0}) = 0$  is approached *non-uniformly* in  $t$ . Indeed, a solution starting with an arbitrarily small energy does initially behave like  $q_{\text{lin}}(t; \vec{z}_i)$  [Eq. (6)]. If the solution is a BOWL solution, an exponentially increasing envelope  $\exp(\omega t)$  will certainly drive  $|q(t; \vec{z}_i)|$  toward the nonlinear regime, and make the amplitude fit the value  $Q^*$  the first time at the instant  $T^*(\vec{z}_i)$ . What happens is that the shortest time  $T^*(\vec{z}_i)$  for fitting  $Q^*$  does diverge in the limit of small initial energy, i.e.,  $\lim_{|\vec{z}_i| \rightarrow 0} T^*(\vec{z}_i) = \infty$ .

An energy scale  $E_l$  determining the low-energy regime for the initial energy  $E_i$  can be obtained as follows. For the system to behave, initially, as a linear oscillator, the energy  $E_i$  must be small compared to the nonlinear energy at  $q = Q^*$ . Hence, from Eq. (17), the low-energy regime can be determined by the condition

$$\text{Low energy: } E_i \ll E_l \equiv \frac{1}{\gamma} \left( \frac{\omega}{2\phi_M \alpha^{2/\gamma}} \right)^{\gamma/(\gamma-2)}. \quad (19)$$

In order to test the validity of the preceding arguments, we have numerically solved [19] the nonlinear Mathieu equation, characterized by a cosine fluctuating frequency

$$\Omega^2(t) = 1 - \xi \cos\left(\frac{2\pi t}{\tau}\right). \quad (20)$$

We have fixed  $t_i = 0$ ,  $\gamma = 4$ , and  $\xi = 10^{-1}$  and tuned the period  $\tau$  in order that the EI conditions are satisfied in the ‘‘gaps’’ of Eq. (20) [20]. The result reported in Fig. 1(a) shows that, in the low-energy regime, the BOWL solutions’ energy exhibits a peaklike envelope. The maximum energy  $E_{\text{Max}}(\vec{z}_i)$ , attained by the oscillator at the peaks’ top, can be studied as a function of  $\vec{z}_i$ , by passing to a polar coordinate system  $(E_i, \theta_i)$ , in which the angle is measured from the  $\dot{q}_i$  axis and  $E_i$  essentially measures  $|\vec{z}_i|^2$ . Figure 1(b) shows that

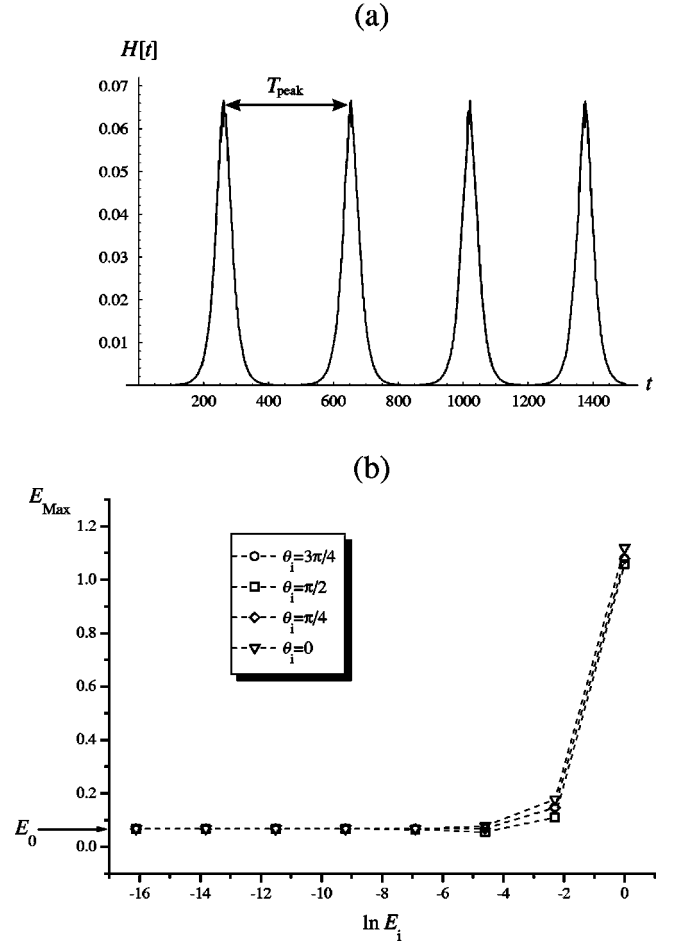


FIG. 1. (a) Time evolution of the energy of a BOWL solution with  $E_i = 5 \times 10^{-7}$  and  $\theta_i = 0$  (low-energy regime). (b)  $E_{\text{Max}}$  vs  $\ln E_i$  for various choices of  $\theta_i$ .  $E_{\text{Max}}$  is calculated on averaging the values of all the maxima observed during the different evolutions, and the corresponding standard deviation is always within the symbols size. The arrow on the left indicates the numerical estimate  $E_0 = 6.66 \times 10^{-2}$ , and the dashed lines are guides for the eye. Selected values are  $\alpha = 1$  and  $\tau = 3.145029$  (the center of the first gap having an exponential rate  $\omega = 2.49757 \times 10^{-2}$ ). Here and in the next figures, all quantities are dimensionless.

$$\lim_{|\vec{z}_i| \rightarrow 0} E_{\text{Max}}(\vec{z}_i) = E_0 > 0 \quad \text{independent of } \theta_i, \quad (21)$$

i.e., the limiting energy  $E_0$  is independent of the initial conditions. We have evaluated  $E_0$  numerically for different choices of  $\alpha$ , performing the calculation both for the first and for the second gap of Eq. (20). The estimate  $\alpha E_0 / \omega \approx 2.66$  (with a deviation in the last significant digit) suggests that, for  $\gamma = 4$ , a convenient scaling quantity should be  $\alpha \times \text{energy} \times \omega^{-1}$ . While the dependence on  $\alpha$  is fully justified on the basis of straightforward scaling arguments (Ref. [21], p. 61), the dependence on  $\omega$  is not as easy to find. From Eq. (19) one can introduce a nonuniversal ( $\omega$ -dependent) proportionality factor  $\varepsilon$  through

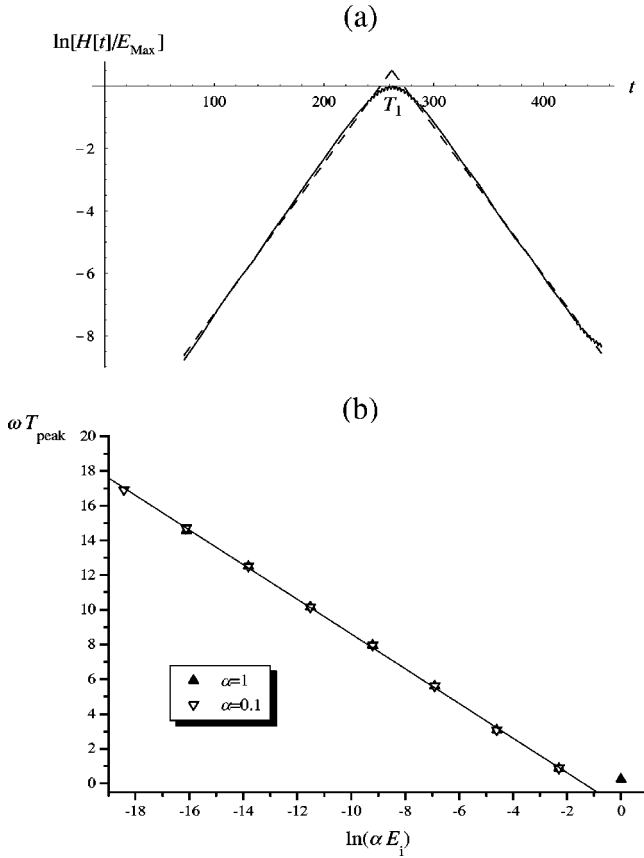


FIG. 2. (a) Detail of the first peak of Fig. 1(a): The natural logarithm of the energy normalized to  $E_{\text{Max}} = 6.666 \times 10^{-2}$  is plotted vs the time  $t$ , around  $T_1 = 262.6$ . The dashed straight lines represent left- and right-hand best fits  $A_{L,R}t + B_{L,R}$ . The slopes  $A_{L,R} = \pm 5 \times 10^{-2}$  and the offsets  $B_L = -12$  and  $B_R = 13$  confirm (with an error  $< 10\%$ ) the exponential shape  $E_{\text{Max}} \exp(-2\omega|t - T_1|)$ . (b)  $\omega T_{\text{peak}}$  vs  $\ln(\alpha E_i)$  for  $\theta_i = \pi/2$  and for two choices of  $\alpha$ . The value of  $T_{\text{peak}}$  is calculated as twice the distance between the first peak  $T_1$  and  $t_i = 0$  (this is correct because at low energies the energy envelope starts essentially in a minimum). The straight lines represent the two best fits, and the overall universal behavior can be summarized as  $\omega T_{\text{peak}} \approx b - a \ln(\alpha E_i)$ , with  $b = -1.4 \pm 0.1$  and  $a = 1.00 \pm 0.01$ . The period  $\tau$  has the same values as in Fig. 1.

$$E_0 = \frac{\varepsilon}{\gamma} \left( \frac{\omega}{2\phi_M \alpha^{2/\gamma}} \right)^{\gamma/(\gamma-2)} \gg E_i. \quad (22)$$

For  $\gamma = 4$ , the numerical data reported in Fig. 1 yield  $\varepsilon \approx 1.71 \times 10^3$ .

The detailed shape of the peaks, reported in Fig. 2(a), shows that the expression  $E_{\text{Max}} \exp(-2\omega|t - T_n|)$  fits the numerical data very well, except in a small interval  $\Delta \tau_{\text{nl}}$ , just around the peak's top. Furthermore, the recurrence of peaks is almost periodic, i.e.,  $T_n = nT_{\text{peak}} + \delta T_n$ , with  $|\delta T_n| \ll T_{\text{peak}}$ . The average period  $T_{\text{peak}}$  is studied in Fig. 2(b) as a function of  $E_i$  and  $\omega$ . The expression

$$T_{\text{peak}} = \omega^{-1} \ln(E_{\text{Max}}/E_i) \quad (\text{low energy}) \quad (23a)$$

also fits the numerical data well, in the low-energy regime [Eq. (19)]. From Eq. (21), it is immediately seen that

$$\lim_{E_i \rightarrow 0} T_{\text{peak}}(E_i) = \omega^{-1} \lim_{E_i \rightarrow 0} \ln(E_0/E_i) = \infty, \quad (23b)$$

i.e., the average period spanning the exponential peaks diverges *logarithmically* in the limit of vanishing initial energy.

The numerical results just described can be interpreted on a physical ground. If the initial energy is low [Eq. (19)], the oscillator spends most of the time in the linear regime described by Hamiltonian (1). This explains the exponential shape of the peaks, which is clearly due to the assumed EI. In the time intervals  $\Delta \tau_{\text{nl}}$ , just around the top of the peaks, the nonlinear term has a highly nonperturbative effect, switching the oscillator from an exponentially increasing component  $f_+$  of the *linear* motion, to an exponentially decreasing one  $f_-$ . Hence the oscillator switches between alternate processes of absorption and dissipation of the energy. It is clearly seen that the energy does increase on average to well above the initial value. If  $\Delta \tau_{\text{nl}} \ll T_{\text{peak}}$ , the process of absorption and dissipation of the energy is almost periodic. In fact the exponential increase of the energy's envelope from  $E_i$  to  $E_{\text{Max}}$  is rapidly followed by a *symmetrical* exponential decrease from  $E_{\text{Max}}$  to  $E_i$ , that takes about the same time. Then the results of Eqs. (23) follow from the equation  $E_{\text{Max}} = E_i \exp(\omega T_{\text{peak}})$ , on assuming that the value  $E_{\text{Max}} \propto q_{\text{Max}}^2$  is attained in an essentially linear regime.

We conclude the present section by stressing that the limiting value  $E_0$  [Eq. (22)] is an important quantity for practical applications concerned with the *catastrophic* behavior of certain macroscopic systems described by Eq. (3) (for example, the horizontal elastic bar with longitudinal time-varying forces). Such systems are characterized by an energy scale  $E_{\text{irr}}$ , marking the onset of some *irreversible* process (viscous flow, fracture, etc.). Since  $E_0$  is the maximum energy attained by a BOWL solution in the limit of *vanishing* initial energy, the condition  $E_0 \ll E_{\text{irr}}$  ensures that the system is always in a ‘‘safe’’ regime, even if some external influence does slightly remove it from the equilibrium state. Instead, the condition  $E_0 \approx E_{\text{irr}}$  corresponds to a ‘‘dangerous’’ regime, in which even an arbitrarily small deviation from the equilibrium state can produce catastrophic effects. It should be noticed that the safety (or nonsafety) condition, expressed in terms of  $E_0$ , is an *intrinsic* property of the system, since  $E_0$  does *not* depend on the initial conditions.

## V. TIME REVERSAL AND THE BOUNDEDNESS OF $S_\omega$

In Sec. III, a question was left open, concerning the boundedness of the curve  $S_\omega$  [Eq. (13)]. The results of Sec. IV can now be used to make the following statement:

*Statement 2:* If  $\Omega^2(-t) \equiv \Omega_{\text{rev}}^2(t)$  satisfies the same EI conditions as  $\Omega^2(t)$ , and yields the same exponential rate  $\omega$ , then  $S_\omega$  is a bounded set of the initial phase space. Equivalently, the convergence radius of the series expansion (10a) for the vanishing solutions is *finite*. Furthermore, the initial energy of the vanishing solutions on the curve  $S_\omega$  is *bounded from above* by the value  $E_0$  [Eq. (23)].

One should note that the condition on  $\Omega^2(t)$  underlying statement 2 is actually very weak. The simplest way to implement the EI conditions is to take  $\Omega^2(t)$  as a BOWL function. If its fluctuations are *random* the exponential instability in Eq. (1) is ensured, regardless to the amplitude of the fluctuations themselves (see, for instance, Ref. [5]). In the case of *periodicity*, the EI conditions involve the average square frequency  $\Omega_0^2$  [Eq. (4)] and the period of the fluctuation itself, but not the sign of the time [1,3,4]. In these two relevant cases, it is clear that passing from  $\Omega^2(t)$  to  $\Omega^2(-t)$  has no influence at all on the EI conditions and on the exponential rate.

In order to prove Statement 2, let us apply the time-reversal transformation to Eq. (3), on setting  $q_{\text{rev}}(\sigma) = q(-t)$ ,  $\sigma = -t$ . It is clear that the motion equation for  $q_{\text{rev}}(\sigma)$  remains the same as Eq. (3), with the new square frequency  $\Omega_{\text{rev}}^2(\sigma)$ . Though  $q_{\text{rev}}(\sigma)$  is *not* in general a solution of the equation of motion (3), the assumed properties of  $\Omega_{\text{rev}}^2(\sigma)$  make it possible to extend the results of the preceding sections to  $q_{\text{rev}}(\sigma)$  too. In particular, let  $q_{\text{rev}}(\sigma)$  be a BOWL solution with an arbitrarily small initial energy  $E_i$  at  $\sigma_i$ , attaining the maximum energy  $E_{\text{Max}}$  at  $\Sigma_1$ . If we assume  $\Sigma_1$  as the new initial time and take  $q_{\text{rev}}(\Sigma_1)$ ,  $-\dot{q}_{\text{rev}}(\Sigma_1)$  as the new initial conditions, then  $q_{\text{rev}}(-\sigma) = q(t)$  is a solution of Eq. (3), whose energy decays (exponentially) from  $E_{\text{Max}}$  to  $E_i$ . Therefore, in the limit  $E_i \rightarrow 0$ ,  $q(t)$  becomes a *vanishing* solution, with maximum energy  $E_{\text{Max}} \rightarrow E_0$ , as shown in Sec. IV. The initial conditions for  $q_{\text{rev}}(\sigma)$  are arbitrary, apart from taking  $E_i$  smaller and smaller. Hence the preceding argument can be applied to construct *any* vanishing solution. This leads immediately to the Statement 2. In particular, this implies that the solutions are necessarily BOWL solutions, if  $E_i > E_0$ . Therefore, the nonlinear term in Eq. (3) acts as a limiting mechanism both for the energy *adsorbed* from the environment and for the energy *dissipated* into the environment.

The analytical construction of the curve  $S_\omega$ , based on Eqs. (10a) and (13), is far from easy. In Sec. VI we will use the *critical* properties of the BOWL-to-vanishing transition to implement the numerical calculation of  $S_\omega$ .

## VI. CRITICAL DYNAMICS: BOWL-TO-VANISHING TRANSITION

A critical process is usually related to the divergence of a certain ‘‘correlation length’’ characteristic of the system. In the case of the BOWL-to-vanishing transition, such a correlation length is related to the (average) recurrence time  $T_{\text{peak}}$  between the peaks of the BOWL solutions (Sec. IV). A special example has been already given by Eq. (23b), showing that the recurrence time does actually diverge logarithmically when the BOWL solutions approach the special vanishing solution  $q_\omega(t) = 0$ . However, it is clear that the divergence of  $T_{\text{peak}}$  is not limited to the case  $E_i \rightarrow 0$ . If a BOWL solution does approach a vanishing solution, its *minimum* energy must vanish. On taking the initial time in this minimum, the fundamental Statement 1 ensures that the next maximum will be split off by larger and larger time intervals. Hence the

divergence of  $T_{\text{peak}}$  is a general feature of the transition. This provides a method for constructing the curve  $S_\omega$  of the initial points of the vanishing solutions, starting from the BOWL solutions. In fact, we can now write  $S_\omega$  as follows:

$$S_\omega = \{ \vec{z}_c ; \lim_{\vec{z}_i \rightarrow \vec{z}_c} T_{\text{peak}}(\vec{z}_i) = \infty \}. \quad (24)$$

There is a practical convenience in adopting Eq. (24) for numerical calculations. In fact, due to the finite precision of the machine, it is virtually impossible to find the exact initial conditions for the vanishing solutions, and draw the curve  $S_\omega$  directly. In practice, all numerical calculations yield, automatically, BOWL solutions, if extended to sufficiently long times.

A general problem in the numerical study of the critical transitions, is to make the *universal* properties emerge in a clear way. If the critical points are not known exactly, this may be a quite difficult task. In the present case, however, the preceding arguments suggest that the *exact* critical behavior of  $T_{\text{peak}}$  is

$$T_{\text{peak}}(E_i) = T_0(E_c) + \omega^{-1} \ln \left( \frac{E_c}{|E_i - E_c|} \right) \quad (E_i \rightarrow E_c) \quad (25)$$

if  $E_c$  is any finite energy on the critical curve  $S_\omega$ . Equation (25) is just a generalization of Eq. (23b). It is customary to express the universal properties of a critical transition through a ‘‘critical exponent’’  $a$  expressing the divergence of some physical quantity, when the ‘‘relevant field’’  $R$  approaches a critical value  $R_c$ . A suitable rescaling can be used to set  $R_c = 0$ . On defining  $R \equiv |E_i - E_c|/E_c$ , Eq. (25) yields

$$\exp(\omega T_{\text{peak}}) \propto R^{-a}, \quad a = 1. \quad (26)$$

The ‘‘principal critical exponent’’ of the BOWL-to-vanishing transition is therefore  $a = 1$ , if we define  $\exp(\omega T_{\text{peak}})$  as the ‘‘correlation length.’’

For the nonlinear Mathieu equation (20), the numerical construction of the curve  $S_\omega$  is reported in Fig. 3(a). The method based on Eq. (24) is useful to locate the points of  $S_\omega$  with any required precision. However, if the square frequency is *periodic* [ $\Omega^2(t) = \Omega^2(t + \tau)$ ], a more rapid method can be used to obtain a rougher estimate of  $S_\omega$  from which an accurate calculation can be started [Fig. 3(b)]. This method is described in the Appendix. In Fig. 3(a) we also report two analytical evaluations, performed at first and second order, of the series expansions (10a) and (13). It is seen that the agreement between numerical and analytical results actually improves with increasing order of approximation. However, the small improvement from first to second order, indicates that the convergence of the series is probably very slow. As expected from Statement 2, the curve  $S_\omega$  is bounded and symmetric with respect to the axis. In fact, the square frequency

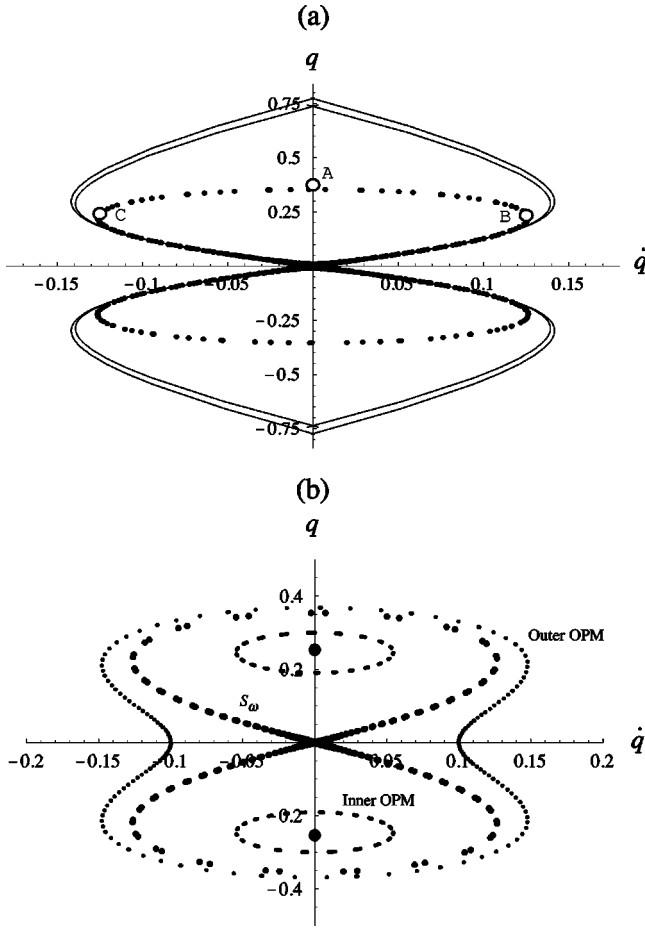


FIG. 3. (a) Construction of  $S_\omega$  in the initial phase space. Points represent numerical values. The outer and inner lines are first- and second-order approximations based on expansion (10a), respectively. Selected values for  $\alpha$  and  $\tau$  are the same as in Fig. 1. Open circles indicate the three critical points considered in Figs. 4 and 6. (b) An alternative numerical method, based on one-period maps (OPM's). For details, see the Appendix.

in Eq. (20) is an *even* function of the time, so that  $\Omega_{\text{rev}}^2(t) = \Omega^2(t)$ . In Figs. 4(a) and 4(b), the numerical check of Eqs. (25) and (26) is reported, close to some critical points  $\vec{z}_c \neq (0,0)$ . The results obtained on the BOWL-to-vanishing transition can be now summarized as follows, in the language of critical phenomena.

(A) The transition is characterized by the logarithmic divergence of the peak-to-peak recurrence time  $T_{\text{peak}}$ . The “critical points”  $\vec{z}_c$  are the initial conditions yielding vanishing solutions, that form a *closed curve*  $S_\omega$  [Fig. 3(a)].

(B) The divergence of  $T_{\text{peak}}$  is *universal*. Choosing  $R \equiv |E_i - E_c|/E_c$  as the “relevant field” of the transition, one sees that the divergence of  $\exp(\omega T_{\text{peak}})$  is characterized by a “critical exponent”  $a=1$  [Figs. 2(b), 4(a) and 4(b)]. The quantity  $\exp(\omega T_{\text{peak}})$  can be regarded as the “correlation length” of the system.

Another simpler way to look at the BOWL-to-vanishing transition follows from using the quantity

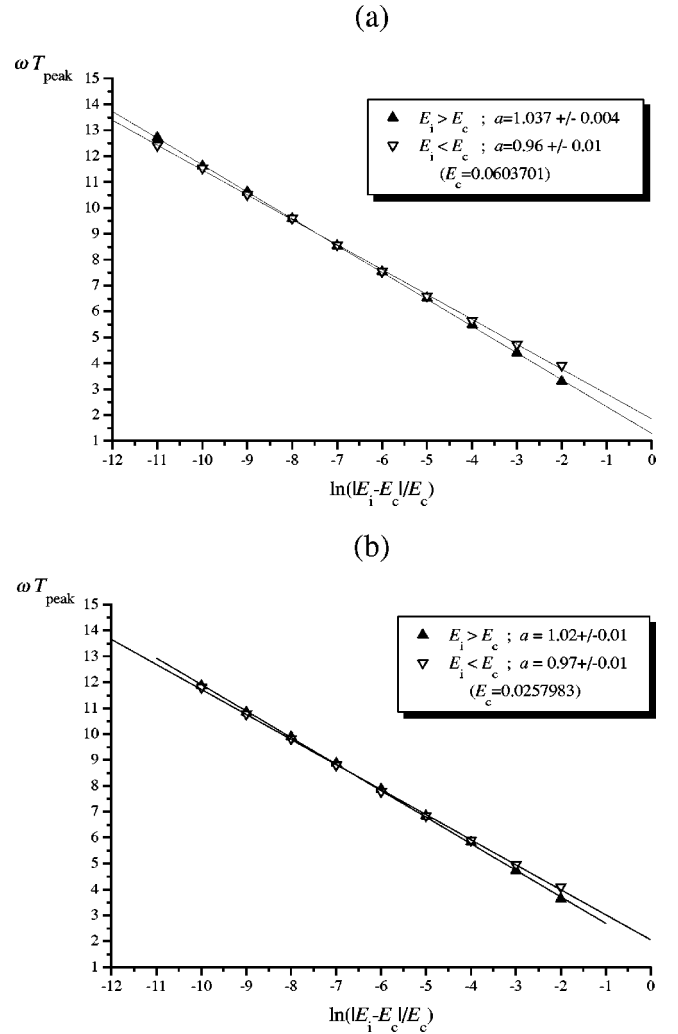


FIG. 4. (a) and (b) Numerical tests of Eq. (27) about points A, B, and C of Fig. 3, respectively. Plot (a) has been obtained on varying  $q_i$  at fixed  $\dot{q}_i=0$  (point A). Plot (b) has been obtained on varying  $\dot{q}_i$  at fixed  $q_i = \pm 0.19809$  (points B and C). In both cases (a) and (b), the linear slope is slightly larger than 1 for  $E_i > E_c$ , and slightly smaller than 1 for  $E_i < E_c$ . However the mean slope is just  $a=1$ , within the errors. We have checked that this compensation effect stems from the evaluation of  $E_c$ , and can be reduced by tuning  $E_c$  more and more exactly. Selected values for  $\alpha$  and  $\tau$  are the same as in Fig. 1.

$$E_\infty(\vec{z}_i) \equiv \limsup_{t \rightarrow \infty(t, \infty[} H(p(t; \vec{z}_i), q(t; \vec{z}_i), t) \quad (27)$$

as the “marker” of the transition. From the fundamental Statement 1, one immediately obtains the following property.

(C) The upper limit  $E_\infty(\vec{z}_i)$ , of the energy in the interval  $(t, \infty[$  for  $t \rightarrow \infty$ , has a *finite-jump discontinuity*  $\Delta E_{\text{jump}} \geq E_{\text{inf}}$  at the transition.

In fact, Statement 1 ensures that  $E_\infty(\vec{z}_i) \geq E_{\text{inf}} > 0$  for each  $\vec{z}_i \in S_{\text{Bowl}}$ . In particular, one has  $E_\infty(\vec{z}_i) \geq E_{\text{inf}}$  even if  $\vec{z}_i$  approaches  $\vec{z}_c \in S_\omega$  from  $S_{\text{Bowl}}$ . However, it is obvious from definition (27) that  $E_\infty(\vec{z}_c) = 0$ , since  $\vec{z}_c$  is the initial point of a vanishing solution.

## VII. HIGH-ENERGY REGIME

The boundedness theorem proven in Ref. [1] has an important consequence on the high-energy treatment of Eq. (3). Since the autonomous term ensuring the boundedness diverges more than linearly with the coordinate, the nonautonomous *linear* term is relatively small when the oscillator amplitude (energy) is large. Therefore, when the amplitude is large (small velocity), the time variation of  $\Omega^2(t)$  is a *small* effect. However, when the amplitude is small, the *velocity* is large, which implies a short action time of the nonautonomous term and an *adiabatic* effect resulting from the time-variation of  $\Omega^2(t)$ . From what we have seen above, in the high-energy regime the solutions of Eq. (3) are characterized by a frequency of oscillation large compared to the *maximum* rate of change  $\nu_{\text{Max}} = |\dot{\Omega}(t)/\Omega(t)|_{\text{Max}}$ . In contrast to the low-energy case, the oscillator now spends most of its time in a nonlinear regime, with a practically constant linear term  $\Omega_{\text{eff}}^2 q$  (adiabatic effect). The remaining linear part  $[\Omega_0^2(1 + \xi(t)) - \Omega_{\text{eff}}^2]q$  acts just as a perturbation (small effect). A nontrivial problem is that the effective square frequency  $\Omega_{\text{eff}}^2$ , yielding the adiabatic effect, is an unknown of the problem, to be found self-consistently. The unperturbed solution, oscillating with large frequency, is therefore given by Eq. (5). An energy scale determining the high-energy regime can be found self-consistently. Let  $\Omega_{\text{nl}}(E_i)$  be the frequency of the solution of the unperturbed equation (5). Since the equation is nonlinear,  $\Omega_{\text{nl}}(E_i)$  is an increasing function of the energy  $E_i$ . The high-energy condition reads  $\Omega_{\text{nl}}(E_i) \gg \nu_{\text{Max}}$ , or, equivalently,

$$\text{High-energy: } E_i \gg E_h, \quad \Omega_{\text{nl}}(E_h) = \nu_{\text{Max}}. \quad (28)$$

Under condition (28), one expects that the exponential instability of the linear Hamiltonian (1) is quite marginal (while it was crucial in the low-energy regime).

According to Eqs. (4) and (5), we introduce a perturbation series

$$q(t) = q_0(t) + \sum_{n=1}^{\infty} q_n[\xi, t], \quad (29)$$

where now the  $q_n[\xi, t]$ 's are *n*th-order *functionals* of  $\xi(t)$ , explicitly depending on the time. A recurrence integral relation does actually connect  $q_n$  to the lower-order terms. In particular,

$$\begin{aligned} q_1[\xi, t] = & -\Omega_0^2 \int_{t_i}^t dt' \Psi(t, t') q_0(t') \xi(t') \\ & + (\Omega_{\text{eff}}^2 - \Omega_0^2) \int_{t_i}^t dt' \Psi(t, t') q_0(t'). \end{aligned} \quad (30)$$

The kernel  $\Psi(t, t') = g_+(t)g_-(t') - g_-(t)g_+(t')$  in Eq. (30) is expressed in terms of two independent solutions of the linear equation

$$\ddot{g} + [\Omega_{\text{eff}}^2 + \alpha(\gamma - 1)|q_0(t)|^{\gamma-2}]g = 0, \quad (31) \quad \text{and}$$

such that  $\dot{g}_+(t)g_-(t) - \dot{g}_-(t)g_+(t) = 1$ . Iterating this procedure to higher orders is a complicated task in general. For the moment, we wish to stress that the first term in the left-hand side member of Eq. (30) is a linear functional of  $\xi(t)$ . If  $\xi(t)$  is a *random-varying* function of time, this term will introduce a chaotic element in the high-energy dynamics. This remark is important for the discussion on the transition to chaos (Sec. IX).

From the above, one expects that, at a high initial energy, the oscillator energy remains almost constant during the time evolution, with fluctuations of order  $\xi(t)$ . To see this, we rely on the canonical perturbation theory [22]. We separate the complete nonautonomous Hamiltonian (2) into an autonomous, nonlinear part

$$H_{\text{anl}} = \frac{p^2}{2} + \Omega_0^2 \frac{q^2}{2} + \frac{\alpha}{\gamma} |q|^\gamma, \quad (32)$$

plus a fluctuating perturbation  $\Omega_0^2 \xi(t)/2q^2$ . The aim is to find, order by order, a canonical transformation to the action-angle variables  $(J, \vartheta)$  such that the new Hamiltonian depends only on  $J$ . In this way,  $J$  is a conserved quantity (an invariant), and  $\vartheta$  evolves linearly in time, with rate  $\partial\mathcal{H}/\partial J$  (if  $\mathcal{H}$  is the new Hamiltonian at the order of interest). Even at first order, the Fourier coefficients of the generating function of the canonical transformation are affected by the problem of the ‘‘secularities,’’ namely, the existence of small denominators typical of nonlinear problems. Special techniques to avoid the divergence of the perturbative terms have been developed. In particular, here we recall the *global removal of resonances* [22], and a recent method proposed by Lewis and co-workers [23,24] specifically constructed within the invariant theory. It is the removal of the secularities that leads one to introduce an effective self-consistent frequency  $\Omega_{\text{eff}}$ , as in Eqs. (5), (30), and (31), essentially driving the denominators out of the resonance conditions.

The explicit form of the first-order results (Hamiltonian, action, frequency, etc.) depends on the Fourier coefficients of the perturbation and on the zero-order action-angle variables. In Appendix C of Ref. [21] these are worked out (for even  $\gamma$ ) in terms of generalized Jacobi elliptic functions. In the case  $\gamma=4$ , one deals with standard Jacobi functions [25]. The relationship between the old action and the new action-angle variables is given in Eq. (4.26) of Ref. [21] for a generic periodic frequency fluctuation. In the special case of the Mathieu problem [Eq. (20)], the time evolution of the zero-order action  $J_0$  can be written in terms of a first-order *conserved* action  $J$ ,

$$J_0(t) = J - \xi \mathcal{A} \mathcal{F}(t), \quad (33)$$

where  $\mathcal{A}$  measures the effective strength of the perturbation

$$\mathcal{A} = \frac{2H_{\text{anl}}(1 - \kappa)|\mathcal{Q}(-\kappa)|}{\kappa \mathcal{K}^2(-\kappa)\Omega_0^2} \frac{\pi\tau}{v^2 - 1}, \quad (34)$$



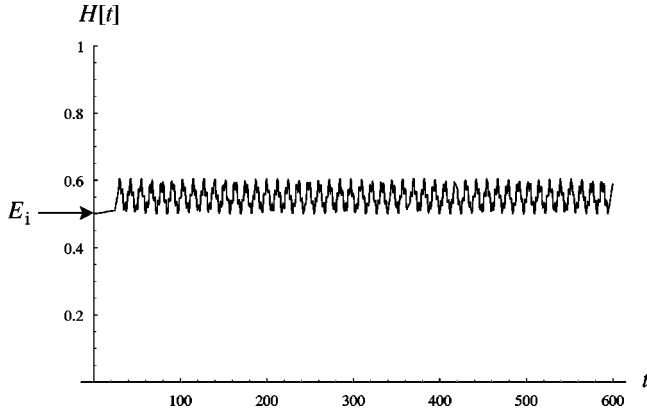


FIG. 5. High-energy fluctuations of a BOWL solution. Selected values for  $\alpha$  and  $\tau$  are the same as in Fig. 1.

$$\mathcal{F}(t) = \frac{v-1}{2} \cos[2\vartheta_i + \bar{\omega}(v+1)t] + \frac{v+1}{2} \cos[2\vartheta_i + \bar{\omega}(v-1)t], \quad (35)$$

$$\bar{\omega} = \frac{2\pi}{\tau}.$$

In Eq. (34),  $K$  indicates the complete elliptic integral of the first kind and  $Q(-\kappa) = \exp[-\pi K(1+\kappa)/K(-\kappa)]$  [25], with

$$\kappa = \frac{\sqrt{\Omega_0^4 + 4\alpha H_{\text{anl}} - \Omega_0^2}}{\sqrt{\Omega_0^4 + 4\alpha H_{\text{anl}} + \Omega_0^2}}. \quad (36)$$

In Eq. (35),  $\vartheta_i$  denotes the initial first-order angle, that evolves with the nonlinear frequency

$$\Omega_{\text{nl}} = \frac{\Omega_0}{\sqrt{1-\kappa}} \frac{\pi}{2K(-\kappa)}. \quad (37)$$

Equation (37) also determines the parameter  $v = \tau\Omega_{\text{nl}}/\pi$ . The relationship between  $J_0$  and  $H_{\text{anl}}(p, q)$  turns out to be

$$J_0 = \frac{4H_{\text{anl}}}{3\Omega_0\pi} \sqrt{1-\kappa} \frac{(1+\kappa)K(-\kappa) - (1-\kappa)E(-\kappa)}{\kappa}, \quad (38)$$

where  $E$  is the complete elliptic integral of the second kind [25]. From Eqs. (38) and (33) it is seen that the oscillator energy is almost constant, with small oscillations of order  $\xi$  (see Fig. 5). Moreover, from Eq. (35) it follows that these oscillations have a quasiperiod  $\tilde{T} = \tau/(v-1)$ , where the two cosines in Eq. (35) have a maximum constructive interference  $\mathcal{F}_{\text{Max}} \approx v$ .

### VIII. A QUANTUM ANALOG OF EQ. (3): CHRONOLOGICAL HUMPS AND SELF-TRAPPED POLARONS

The stationary Schrödinger equation

$$\frac{1}{2} \frac{d^2\psi}{dx^2} + [\epsilon - V(x)]\psi + \frac{\alpha}{2} |\psi|^{\gamma-2}\psi = 0 \quad (m = \hbar = 1) \quad (39)$$

is formally equivalent to Eq. (3), if the time is read as a spatial coordinate  $x$ , and  $q(t)$  is replaced by the wave function  $\psi(x)$ . The average value  $\Omega_0^2$  of the square frequency [Eq. (4)] plays the role of (twice) the energy eigenvalue  $\epsilon$ , and the fluctuating part of  $\Omega^2$  then becomes an external potential. The nonlinear term can in turn be read as an *attractive* potential energy multiplied by the wave function. In Eq. (39) the attractive energy is a homogeneous function of the probability density of the quantum particle, i.e., the particle is assumed to undergo a sort of self-attraction. This model-system is actually well known in condensed matter physics [26]. It describes a charged particle (the *polaron*) in a strongly polarized medium, approximated by a uniform “jellium.” The potential energy  $V(x)$  can be regarded as the nonpolarized part of the host lattice. For example, if  $\Omega^2$  in Eq. (3) is *periodic*, its quantum analog [Eq. (39)] describes a polaron in a one-dimensional *crystal* of nonpolarized objects. If  $\psi(x)$  vanishes to  $\pm\infty$ , one has the so-called “self-trapped polaron.”

The notion of self-trapped polaron can be applied to Eq. (3) too, by extending the definition of  $\Omega^2(t)$  to any  $t < t_i$ . The integral form of Eqs. (9) can indeed be “time reversed,” under the weak conditions underlying Statement 2. Therefore, an expansion like Eq. (10a) can be found even for a solution vanishing at  $t = -\infty$ . The matching of the two vanishing branches at  $t_i$  determines in general isolated points in the initial phase space, which are functions of  $\Omega_0^2$ . The normalization of the solution would finally solve the eigenvalue *quantum* problem for  $\Omega_0^2$ . In the *classical* problem, however, no normalization is required, and  $\Omega_0^2$  is a fixed arbitrary quantity. The above simply outlines the existence of special initial conditions at  $t_i$ , such that the solution has zero amplitude at  $t = -\infty$ , increases exponentially (in envelope) up to a maximum, then vanishes again at  $t = +\infty$ . We call this solution a “chronological hump,” to distinguish it from the self-trapped polaron. We stress that the existence of chronological humps for  $\Omega_0^2 > 0$  is far from trivial, and is closely related to the *fluctuating* part of the square frequency. To see this, the quantum analog [Eq. (39)] is again convenient. If  $V(x) = 0$ , in fact, the energy eigenvalue  $\epsilon$  of the self-trapped polaron would be certainly *negative*. The positive part of the spectrum would correspond to plane-wave states (mobile polarons) only. However, if  $V(x)$  is *periodic*, the spectrum in the absence of the self-attracting term is characterized by “gaps” of finite width, spanning the “bands” of allowed energy values (the Bloch theorem). Gaps exist above any arbitrarily large *positive* value of the energy. At this stage, the self-attractive term can be regarded as a “defect” in a

crystal. The typical effect of a defect in a band-spectrum is to produce localized levels in the gaps. This explains why a fluctuating  $V(x)$  in Eq. (39) may yield self-trapped polarons even in the *positive* part of the spectrum. Coming back to the classical problem, we can conclude that, for  $\xi(t)=0$ , a chronological hump can exist only if  $\Omega_0^2 < 0$ . Then, in the case  $\Omega_0^2 > 0$ , a *nonzero* time fluctuation of the square frequency is a *necessary* condition for the existence of chronological humps.

The chronological humps are closely related to the BOWL-to-vanishing transition studied in Sec. VI. To see this, let us consider a BOWL solution at low energy (Sec. IV) and the center  $T_1$  of the first peak [Fig. 2(a)], in which the energy attains the maximum value  $E_{\text{Max}}$ . For  $t > T_1$ , the energy decreases exponentially for a time interval comparable with  $T_{\text{peak}}/2$ . Taking smaller and smaller values of the initial energy, we have seen that both  $T_1 \geq T^*(\vec{z}_1)$  and  $T_{\text{peak}}$  become diverging large [Eqs. (23)], while  $E_{\text{Max}}$  tends to  $E_0$ . If we “follow” the peak’s shift to  $+\infty$ , we find a limit solution vanishing in both directions of time (now referred to as  $T_1$ ) and attaining a maximum energy  $E_0$ . A solution of this kind is nothing but a chronological hump. Hence, for  $E_i \rightarrow 0$ , it is seen that the divergence of  $T_{\text{peak}}$  is also responsible for the appearance of a chronological hump, whose center “runs away” to infinity. In order to see the chronological humps at a *finite* time, one simply has to approach the critical curve  $S_\omega$  in any point  $\vec{z}_c \neq (0,0)$ , and study Eq. (3) and its time-reversed form. In Fig. 6, we show the numerical results obtained in three different critical points  $\vec{z}_c \neq (0,0)$ . The data refer to the energy of the solutions in both directions of time. It is clearly seen that the complete solutions are chronological humps, whose maximum energy  $E_0$  is attained at different *finite* times (in the past or in the future, with respect to  $t_i$ ), depending on the critical initial point  $\vec{z}_c$ . In particular, Fig. 6(a) shows the chronological hump attaining its maximum energy just around the *initial* time.

The BOWL-to-vanishing transition can be now interpreted in a more physical way. The peaks described in Sec. IV at low energy can be regarded as “correlated” chronological humps. The transition simply shifts the chronological humps apart, leaving just one at a finite time, if  $\vec{z}_c \neq (0,0)$ , or leaving none, if  $\vec{z}_c = (0,0)$ . The time scale  $T_{\text{peak}}$  is actually the correlation time between the chronological humps.

Due to the analogy between Eqs. (3) and Eq. (39), these results are relevant for the polaron problem too. In particular, all the universal aspects of the BOWL-to-vanishing transition (Sec. VI) can be now extended to the transition from *mobile* to *self-trapped* polarons in one spatial dimension.

## IX. CONCLUSIONS

The present paper addresses a special case of generalized oscillator, in which the nonautonomous force is *linear*, with a time-fluctuating strength, while the *autonomous* force increases more than linearly with the amplitude [Eqs. (1) and (3)]. Interest in this problem comes from the interplay between two contrasting mechanisms: the bounding effect of the nonlinear autonomous term [1], and the exponential in-

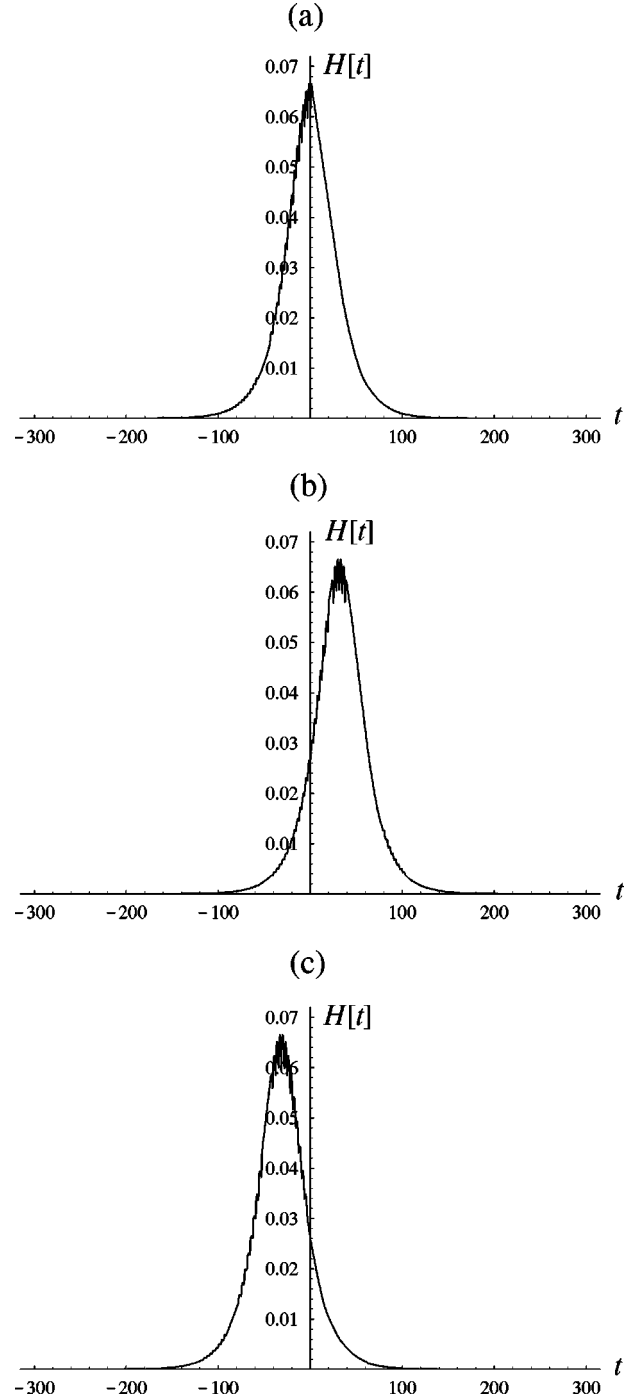


FIG. 6. Evolution, in both directions of time, of the energy of three chronological humps with different initial conditions at  $t_i = 0$ . (a), (b), and (c) refer, respectively, to points A, B, and C in Fig. 3. Selected values for  $\alpha$  and  $\tau$  are the same as in Fig. 1. Note the shifting to the future (b) and to the past (c) of the hump center, with respect to the hump centered about the initial instant (a).

stability (EI) produced by time fluctuations of the linear strength under suitable conditions (EI conditions). If the initial energy  $E_i$  is large enough, the fluctuating part of the strength can be treated as a perturbation (Sec. VII). The resulting solutions are *bounded and oscillating without limit*

(BOWL), and their energy is conserved, apart from relatively small fluctuations (Fig. 5). EI conditions play no essential role in this case.

The situation drastically changes if  $E_i$  is small enough. In this case, EI conditions turn out to be crucial. First, they produce solutions that vanish exponentially in time (Sec. III), whose initial values lie on a closed curve  $S_\omega$  of the initial phase space (Sec. V). The analogy between Eq. (3) and the quantum polaron in one dimension [Eq. (39)], leads one to introduce the *chronological hump* as a classical counterpart of the self-trapped polaron (Sec. VIII). A chronological hump is a solution of Eq. (3) that vanishes exponentially in both directions of the time.

In the low-energy sector (Sec. IV), an alternate absorption-dissipation process characterizes the energy of the BOWL solutions, leading to an almost periodic sequence of peaks, with about the same maximum energy  $E_{\text{Max}}$ . A crucial point is that  $E_{\text{Max}}$  is a function of the initial energy  $E_i$  bounded from below by a strictly positive value  $E_{\text{inf}}$ . The average period  $T_{\text{peak}}(\dot{q}_i, q_i)$ , spanning two successive peaks, is a new characteristic time scale determined by the initial conditions and by  $\omega$  [Eqs. (23b) and (25)]. The quantity  $\omega$  is just the exponential rate of the *unstable* solutions of the linear problem Eq. (1).

The initial locus  $S_\omega$  of the vanishing solutions is a *critical* curve in the initial phase space of points  $\vec{z}_i = (\dot{q}_i, q_i)$ . Moving on a line of initial points connecting BOWL solutions outside and inside  $S_\omega$ , it is shown that  $T_{\text{peak}}$  diverges at the intersection point with  $S_\omega$ . This is what we call the *BOWL-to-vanishing* transition. The transition has a universal character expressed by a ‘‘critical exponent’’  $a = 1$ , and can be regarded as the passage from a sequence of ‘‘correlated’’ chronological humps (BOWL solutions), to a single chronological hump. The larger the time scale  $T_{\text{peak}}$ , the larger the degree of correlation. It is likely that the critical transition just outlined is also associated with the divergence of the high-energy series expansion [Eq. (29)] along the curve  $S_\omega$ . Actually, the existence of a critical boundary between ‘‘inner’’ and ‘‘outer’’ BOWL solutions suggests that the dynamics is basically different inside and outside  $S_\omega$ . An indication of this possibility is given in the Appendix.

In Sec. I, some physical applications of the present results were outlined. Now we briefly discuss a further one, i.e., the Fermi-Pasta-Ulam (FPU) problem [17,18].

The FPU problem is a many-body *autonomous* problem, with linear and nonlinear couplings among first-nearest-neighbor particles, regularly distributed on a chain. Introducing the amplitudes  $A_k(t)$  of the modes with wave vector  $k$ , one obtains a system of nonlinear equations, with all *constant* coefficients:

$$\begin{aligned} \ddot{A}_k + \Omega_k^2 A_k + \alpha_2 \sum_{k_1, k_2} C_{k, k_1, k_2} A_{k_1} A_{k_2} + \dots \\ + \alpha_m \sum_{k_1, \dots, k_m} C_{k, \dots, k_m} A_{k_1} \dots A_{k_m} = 0. \end{aligned} \quad (40)$$

Despite the fact that Eq. (3) is basically different from the

differential problem of Eq. (40), there are some remarkable analogies in the results. First, at high initial energy, the energy of each FPU mode fluctuates about the initial value just like the energy [Eq. (2), Fig. 5]. At low-energy, a peaklike structure is obtained, with a quasiconstant *recurrence time*  $T_{\text{rec}}^{(k)}$  spanning the peaks. This looks very similar to the results obtained in Sec. IV [Fig. 1(a)], in terms of the average period  $T_{\text{peak}}$ . The low-to-high energy transition in the FPU problem is a famous example of *transition to chaos* [18]. To the authors’ knowledge, the nature (smooth or critical) of this transition is still an open question. In the present case, the result of Sec. VI points to a critical transition.

There are motivations suggesting that the analogies just mentioned are *not* casual. Indeed, one possible approach to the FPU problem is transforming the system (40), of *autonomous-coupled* equations, into a set of *decoupled non-autonomous* equations. A method was suggested, leading to decoupled *linear* equations, including a time-dependent forcing, a renormalized linear frequency and an autonomous friction term [27,28]. Our approach is more closely concerned with the non-linear structure of Eq. (40). On extracting terms depending explicitly on  $A_k$ , we write Eq. (40) as follows:

$$\begin{aligned} \ddot{A} + [\Omega_k^2 + D_k^{(1)}(\{A_{k'}\}_{k' \neq k})] A_k + D_k^{(2)}(\{A_{k'}\}_{k' \neq k}) A_k^2 + \dots \\ + D_k^{(m-1)}(\{A_{k'}\}_{k' \neq k}) A_k^{m-1} + \Gamma_k A_k^m = F_k(\{A_{k'}\}_{k' \neq k}), \end{aligned} \quad (41)$$

where the coefficients  $D_k^{(j)}$ ’s and the driving force  $F_k$  depend on time through the other variables  $\{A_{k'}\}_{k' \neq k}$ , while the highest-order coefficient  $\Gamma_k = \alpha_m C_{k, k, \dots, k}$  is *constant*. Our suggestion is to look for a self-consistent approximation replacing the  $D_k^{(j)}$ ’s and  $F_k$  with suitable time-varying functions  $\bar{D}_k^{(j)}(t)$  and  $\bar{F}_k(t)$ . For  $\gamma - 1 = m$  integer and *odd*, the effective equation resulting from Eq. (41) would be

$$\begin{aligned} \ddot{A}_k + [\Omega_k^2 + \bar{D}_k^{(1)}(t)] A_k + \dots + \bar{D}_k^{(\gamma-2)}(t) A_k^{(\gamma-2)} \\ + \Gamma_k A_k^{(\gamma-1)} = \bar{F}_k(t). \end{aligned} \quad (42)$$

This is a generalization of Eq. (3), including time-varying nonlinear terms of lower order, and a time-dependent forcing. Now, let us assume the same ansatz as in Refs. [27,28], i.e., that the mode-mode coupling should produce *random* time-dependent fluctuations in the effective equations. If so, we expect that the fluctuating part  $\bar{D}_k^{(1)}(t)$  of the square frequency is random too. As already discussed in Sec. V, this is a sufficient condition for the EI, independent of the value of  $\Omega_k^2$ . One should note that fitting the EI condition is crucial for the relationship between Eq. (3) and the FPU problem. In fact, it is the EI condition that produces the peak-to-peak recurrence time and all the analogies stressed above. A further important point is that the quasiperiodicity of the peaks in Fig. 1(a) is *not* due to the periodicity of the frequency fluctuation. In fact, Eq. (23a) shows that the average period  $T_{\text{peak}}$  depends essentially on the initial energy and on the exponential rate  $\omega$ . A random fluctuation is thus expected to

yield quasiregular recurrence times, simply because it always produces a nonvanishing  $\omega$ . At high energy, instead, the lowest-order approximation [Eq. (30)] shows that the energy fluctuations are influenced by the same randomness as  $\Omega^2(t)$ . Hence the dynamical equation (3) is an example of a *random-varying* parameter [ $\Omega^2(t)$ ], producing a *nonchaotic* response at low initial energy, and a *chaotic* one at high energy. This suggests that the interplay between EI and nonlinearity studied in the present paper could be a basic mechanism underlying one of the most debated questions in modern classical physics, i.e., the transition to chaos.

#### APPENDIX: NUMERICAL AND ANALYTICAL LOCATION OF $S_\omega$ IN THE PERIODIC CASE

If  $q(t)$  is a solution starting from  $\vec{z}_i = (p_i, q_i)$  at  $t = t_i$  then, in the presence of a frequency fluctuating with period  $\tau$ , the points  $\vec{z}_k = [p(t_i + k\tau), q(t_i + k\tau)]$  give rise to the *same* solution from  $t \geq t_i + k\tau$  ( $k = 1, 2, \dots$ ). In addition, given an invariant  $I[p(t), q(t), t]$  such that  $I(p, q, t) = I(p, q, t + \tau)$ , the points  $\vec{z}_k$  will all belong to a certain level curve of  $I(p, q, t_i)$ . We call the set of points

$$S_\tau[\vec{z}_i] = \{\vec{z}_k \in \mathbb{R}^2; \vec{z}_k = [p(t_i + k\tau), q(t_i + k\tau)], k = 0, 1, 2, \dots, \vec{z}_0 = \vec{z}_i\} \quad (\text{A1})$$

a one-period map (OPM). In particular, if a point on  $S_\tau[\vec{z}_i]$  generates a vanishing solution, then the same will do every point of  $S_\tau[\vec{z}_i]$ . Thus, by definition, every set  $S_\tau$  associated with vanishing solutions is contained in  $S_\omega$ . In other words, we can locate at least some points of  $S_\omega$  by finding a single point on it, following the solution at discrete time steps. This was done in Fig. 3(a) (black points) starting from  $(p_i = -0.0226392, q_i = 0.0232694)$ . As stated in Sec. VI, a suitable starting point to plot  $S_\omega$  can be found by looking at the divergence of the correlation time  $T_{\text{peak}}$ . However, the analysis of several OPM's suggested us an alternative way to locate the points of  $S_\omega$ . We systematically observed the fol-

lowing property: a OPM starting *outside* (*inside*)  $S_\omega$  always remains outside (*inside*). In Fig. 3(b) we report plots corresponding to inner and outer OPM's, together with the numerical location of  $S_\omega$  already shown in Fig. 3(a). It is seen that outer OPM's always fall on (ideal) closed patterns, surrounding  $S_\omega$ . At high energies these patterns have a quasielliptical shape, typical of the level curves of an autonomous nonlinear oscillator (recall Sec. VII). They approach the 8-like structure of  $S_\omega$  from outside, by inflecting themselves more and more along the  $\dot{q}$  axis. The inner OPM's form two symmetrical patterns, inside each lobe of  $S_\omega$ . It is clear that one may locate  $S_\omega$  as the border line separating one-pattern (outer) OPM's from two-pattern (inner) OPM's. An interesting limiting case of two-pattern OPM's is indicated in Fig. 3(b) by the two full circles on the  $q$  axis. Recalling definition (A1), one sees that these two points represent a *periodic* solution with period  $2\tau$ . The existence of periodic solutions with period  $K\tau$  ( $K = 1, 2, \dots$ ) for a class of nonlinear nonautonomous oscillators was proven by Dieckerhoff and Zehnder [29]. In the OPM representation, these particular BOWL solutions would appear as invariant sets of  $K$  distinct points.

Now let us come to analytical estimates of  $S_\omega$  based on the expansion (10a). Essentially, we make use of this series expansion in connection with identity (8). At each order in  $\alpha$  one needs the lower-order terms  $q_j(t)$  to calculate the resulting nested integrals. Then one chooses  $r = q_-$  as a free parameter, and determines  $q_+$  as a function of  $q_-$  through Eq. (8) truncated at some order. For instance, at second order we find

$$q_+ = \alpha L_1 |r|^{\gamma-2} r + \alpha^2 L_2 (\gamma-1) |r|^{2\gamma-4} r, \quad (\text{A2})$$

where  $L_1$  comes from the insertion of the zero-order solution  $q_{-f_-}(t)$ :

$$L_1 = \int_{t_i}^{\infty} dt |u_-(t)|^\gamma e^{-\gamma\omega t}, \quad (\text{A3})$$

and

$$L_2 = \int_{t_i}^{\infty} dt e^{-\omega(\gamma-2)t} |u_-(t)|^{\gamma-2} u_+(t) u_-(t) \int_{t_i}^{\infty} dt' |u_-(t')|^\gamma e^{-\gamma\omega t'} + \int_{t_i}^{\infty} dt e^{-\gamma\omega t} |u_-(t)|^\gamma \int_{t_i}^t dt' |u_-(t')|^{\gamma-2} u_+(t') u_-(t') e^{-\omega(\gamma-2)t'}, \quad (\text{A4})$$

$u_-(t)$  being the oscillating part of  $f_-(t)$ . We have performed this calculation at the center of the first gap of the Mathieu equation (20) (as in Fig. 1) obtaining  $L_1 = 3.52$  and  $L_2 = 0.466$  ( $t_i = 0$ ). At this stage, the results can be plotted in  $(\dot{q}_i, q_i)$  space on using the (nonsingular) linear transformation between  $q_\pm$  [Eq. (6)] and the initial conditions. In Fig. 3 this was done for  $\gamma = 4$  and  $\alpha = 1$ . It should be stressed that Eq. (A2) reproduces only *one* branch of the ‘‘8-like’’ continuous curves of Fig. 3. It is sufficient to time reverse Eqs. (8) and (9) (in the spirit of Secs. V and VIII) to obtain the specular equation ( $\dot{q}_i \rightarrow -\dot{q}_i$ ).

- [1] L. Ferrari and C. Degli Esposti Boschi, *Phys. Rev. E* **62**, R3039 (2000).
- [2] Here and in what follows, the amplitude  $q$ , the momentum  $p$ , the time  $t$ , and the frequency  $\Omega(t)$  will be dimensionless. Passing to the dimensionless form of the equations can be easily done by suitable rescaling operations.
- [3] L. D. Landau and E. M. Lifshitz, *Mechanics* (Pergamon Press, Oxford, 1960).
- [4] N. Bogolioubov and I. Mitropolski, *Les Méthodes Asymptotiques en Théorie des Oscillations Non Linéaires* (Gauthier-Villars, Paris, 1962) (in French). See, in particular, Sec. 17.
- [5] M. Plischke and B. Bergersen, *Equilibrium Statistical Physics*, 2nd ed. (World Scientific, Singapore, 1994).
- [6] I. A. Pedrosa, *Phys. Rev. D* **36**, 1279 (1987).
- [7] J.-Y. Ji and J. K. Kim, *Phys. Rev. A* **53**, 703 (1996).
- [8] H.-C. Kim, M.-H. Lee, J.-Y. Ji, and J. K. Kim, *Phys. Rev. A* **53**, 3767 (1996).
- [9] I. A. Pedrosa, *Phys. Rev. A* **55**, 3219 (1997).
- [10] G. A. Garrett, A. G. Rojo, A. K. Sood, J. F. Whitaker, and R. Merlin, *Science* **275**, 1638 (1997). Also see D. Clery, *ibid.* **275**, 1566 (1997).
- [11] T. Satogata, T. Chen, B. Cole, D. Finley, A. Gerasimov, G. Goderre, M. Harrison, R. Johnson, I. Kourbanis, C. Manz, N. Merminga, L. Michelotti, S. Peggs, F. Pilat, S. Pruss, C. Saltmarsh, S. Saritepe, R. Talman, C. G. Trahern, and G. Tsironis, *Phys. Rev. Lett.* **68**, 1838 (1992).
- [12] Y. Wang, M. Ball, B. Barbson, J. Budnick, D. D. Caussyn, A. W. Chao, J. Collins, V. Derenchuk, S. Dutt, G. East, M. Ellison, D. Friesel, B. Hamilton, H. Huang, W. P. Jones, S. Y. Lee, D. Li, J. Y. Liu, M. G. Minty, K. Y. Ng, X. Pei, A. Riabko, T. Sloan, M. Syphers, Y. T. Yan, and P. L. Zhang, *Phys. Rev. E* **49**, 5697 (1994).
- [13] M. Giovannozzi, W. Scandale, and E. Todesco, *Phys. Rev. E* **57**, 3432 (1998).
- [14] A. Chao, D. Johnson, S. Peggs, J. Peterson, C. Saltmarsh, L. Schachinger, R. Meller, R. Siemann, R. Talman, P. Morton, D. Edwards, D. Finley, R. Gerig, N. Gelfand, M. Harrison, R. Johnson, N. Merminga, and M. Syphers, *Phys. Rev. Lett.* **61**, 2752 (1988).
- [15] O. Brüning, *Part. Accel.* **41**, 133 (1993); DESY Report No. DESY-HERA-92-20 (1992).
- [16] W. Paul, *Rev. Mod. Phys.* **62**, 531 (1990).
- [17] R. Livi, M. Pettini, S. Ruffo, M. Sparpaglione, and A. Vulpiani, *Phys. Rev. A* **31**, 1039 (1985); R. Livi, M. Pettini, S. Ruffo, and A. Vulpiani, *ibid.* **31**, 2740 (1985).
- [18] J. Ford, *Phys. Rep.* **213**, 271 (1992).
- [19] Throughout this work solutions of the ordinary differential equations have been obtained with a commercial software for numerical and symbolic calculus. It switches between an implicit nonstiff Adams method ( $1 \leq \text{order} \leq 12$ ) and a stiff Gear method (backward difference formula,  $1 \leq \text{order} \leq 5$ ). The total integration time [in units fixed by Eq. (20)] was chosen up to  $2 \times 10^3$ , and divided into up to  $4 \times 10^4$  steps. We monitored energies down to  $\sim 10^{-7}$  [in units fixed by Eq. (2)], using up to 18 digits of working precision, and up to ten digits as goal for absolute and relative accuracies.
- [20] The term “gap” is used here in analogy with the Bloch theorem: the EI conditions are indeed equivalent to taking  $\Omega_0^2$  as an energy eigenvalue falling in one gap of a one-dimensional crystal. In the standard notations of the linear Mathieu problem, a fixed  $\xi$  corresponds to an operation line (OL)  $a/q = 2/\xi$  in the parameter space  $(q, a)$ . Consistently, we have set  $\tau$  in the midway point of the segments of intersection between the OL and the gap zones. For a wide treatment of the theory of the Mathieu equation the reader may consult the dedicated chapter in M. Abramowitz and I. A. Stegun, *Handbook of Mathematical Functions: With Formulas, Graphs and Mathematical Tables* (Dover, New York, 1972).
- [21] C. Degli Esposti Boschi, Ph.D. Doctoral thesis, Università degli Studi di Bologna, 2000. The author can provide a PostScript or pdf copy of this document on request.
- [22] A. J. Lichtenberg and M. A. Leiberman, *Regular and Chaotic Dynamics*, 2nd ed. (Springer-Verlag, New York, 1992). See, in particular, Chap. 2.
- [23] H. R. Lewis, J. W. Bates, and J. M. Finn, *Phys. Lett. A* **215**, 160 (1996).
- [24] H. R. Lewis, *Phys. Lett. A* **235**, 581 (1997).
- [25] I. S. Gradshteyn and I. M. Ryzhik, *Table of Integrals, Series and Products: Corrected and Enlarged Edition* (Academic Press, San Diego, 1980).
- [26] T. Holstein, *Ann. Phys. (N.Y.)* **8**, 343 (1959).
- [27] S. Lepri, *Phys. Rev. E* **58**, 7165 (1998).
- [28] S. Lepri, R. Livi, and A. Politi, *Europhys. Lett.* **43**, 271 (1998).
- [29] R. Dieckerhoff and E. Zehnder, *Ann. Sci. Norm. Super. Pisa, Cl. Sci.*, **14**, 79 (1987).